JOURNAL OF GEOPHYSICAL RESEARCH, VOL. 113, D16116, doi:10.1029/2007JD009571, 2008

The frequency and dynamics of stratospheric sudden warmings in the 21st century

A. J. Charlton-Perez,[1] L. M. Polvani,[2] J. Austin,[3,4] and F. Li[3,5]

Received 5 November 2007; revised 26 March 2008; accepted 11 April 2008; published 27 August 2008.

[1] Changes to stratospheric sudden warmings (SSWs) over the coming century, as predicted by the Geophysical Fluid Dynamics Laboratory (GFDL) chemistry climate model [Atmospheric Model With Transport and Chemistry (AMTRAC)], are investigated in detail. Two sets of integrations, each a three-member ensemble, are analyzed. The first set is driven with observed climate forcings between 1960 and 2004; the second is driven with climate forcings from a coupled model run, including trace gas concentrations representing a midrange estimate of future anthropogenic emissions between 1990 and 2099. A small positive trend in the frequency of SSWs is found. This trend, amounting to 1 event/decade over a century, is statistically significant at the 90% confidence level and is consistent over the two sets of model integrations. Comparison of the model SSW climatology between the late 20th and 21st centuries shows that the increase is largest toward the end of the winter season. In contrast, the dynamical properties are not significantly altered in the coming century, despite the increase in SSW frequency. Owing to the intrinsic complexity of our model, the direct cause of the predicted trend in SSW frequency remains an open question.

Citation: Charlton-Perez, A. J., L. M. Polvani, J. Austin, and F. Li (2008), The frequency and dynamics of stratospheric sudden warmings in the 21st century, *J. Geophys. Res.*, *113*, D16116, doi:10.1029/2007JD009571.

1. Introduction

[2] Major midwinter stratospheric sudden warmings (SSWs) are the primary mode of variability in the Northern Hemisphere stratosphere, and play a key role in the coupling between the stratosphere and the troposphere below. SSWs directly impact the chemistry and dynamics of the stratosphere, and have been shown to affect the tropospheric circulation on seasonal timescales [*Baldwin and Dunkerton*, 2001; *Charlton et al.*, 2004]. It is therefore important to understand how changes to atmospheric constituents might affect on the frequency and dynamics of SSWs in the current century, in order to determine if and how changes in stratospheric variability might influence tropospheric climate [e.g., *Scaife et al.*, 2005; *Gillett and Thompson*, 2003].

[3] A limited number of studies have already examined this question and reported mixed results. One method for determining the response of the stratospheric variability to anthropogenic greenhouse gas emissions is to run time-slice experiments, in which climate model integrations with fixed preindustrial carbon dioxide (CO_2) concentrations are compared to integrations with and doubled CO_2 (or greater). Some time-slice studies indicate that SSWs will decrease in a doubled CO_2 climate (e.g., by a factor of 4 in the study of *Rind et al.* [1998]), while others have shown large increases in SSW activity in time-slice integrations (L. J. Gray, personal communication 2008, using the UK Met Office Unified Model). The reported results, however, are often statistically significant only for large changes in CO_2, typically of the order of four times preindustrial concentrations. Several studies have also found a decrease in the strength of the westerly jet associated with the polar vortex in the stratosphere [e.g., *Gillett et al.*, 2003; *Sigmond et al.*, 2004]; these studies have not, however, explicitly examined changes to SSWs.

[4] A second approach consists of running models with time-dependent, observed or predicted concentrations of greenhouse gases, and determining whether significant trends in modelled stratospheric variability result. Only a limited number of experiments of this type have been performed, to date, with stratosphere-resolving General Circulation Models (GCMs) or Chemistry Climate Models (CCMs), owing to the large computational cost involved. *Butchart et al.* [2000] performed a two-ensemble member time-evolving simulation with a stratosphere-resolving model, run between 1992 and 2051. In contrast to the time-slice integrations, they did not report a robust change to the frequency of SSWs; this was due, in part, to the large interdecadal variability in SSW frequency.

[5] In this paper, we examine the frequency of SSWs between the 1960s and 2090s from integrations using the

[1]Department of Meteorology, University of Reading, Reading, UK.
[2]Department of Applied Mathematics and Applied Physics, and Department of Earth and Environmental Sciences, Columbia University, New York, New York, USA.
[3]Geophysical Fluid Dynamics Laboratory, Princeton, New Jersey, USA.
[4]University Corporation for Atmospheric Research, Boulder, Colorado, USA.
[5]Now at Goddard Earth Science and Technology Center, University of Maryland, Baltimore County, Baltimore, Maryland, USA.

0148-0227/08/2007JD009571$09.00

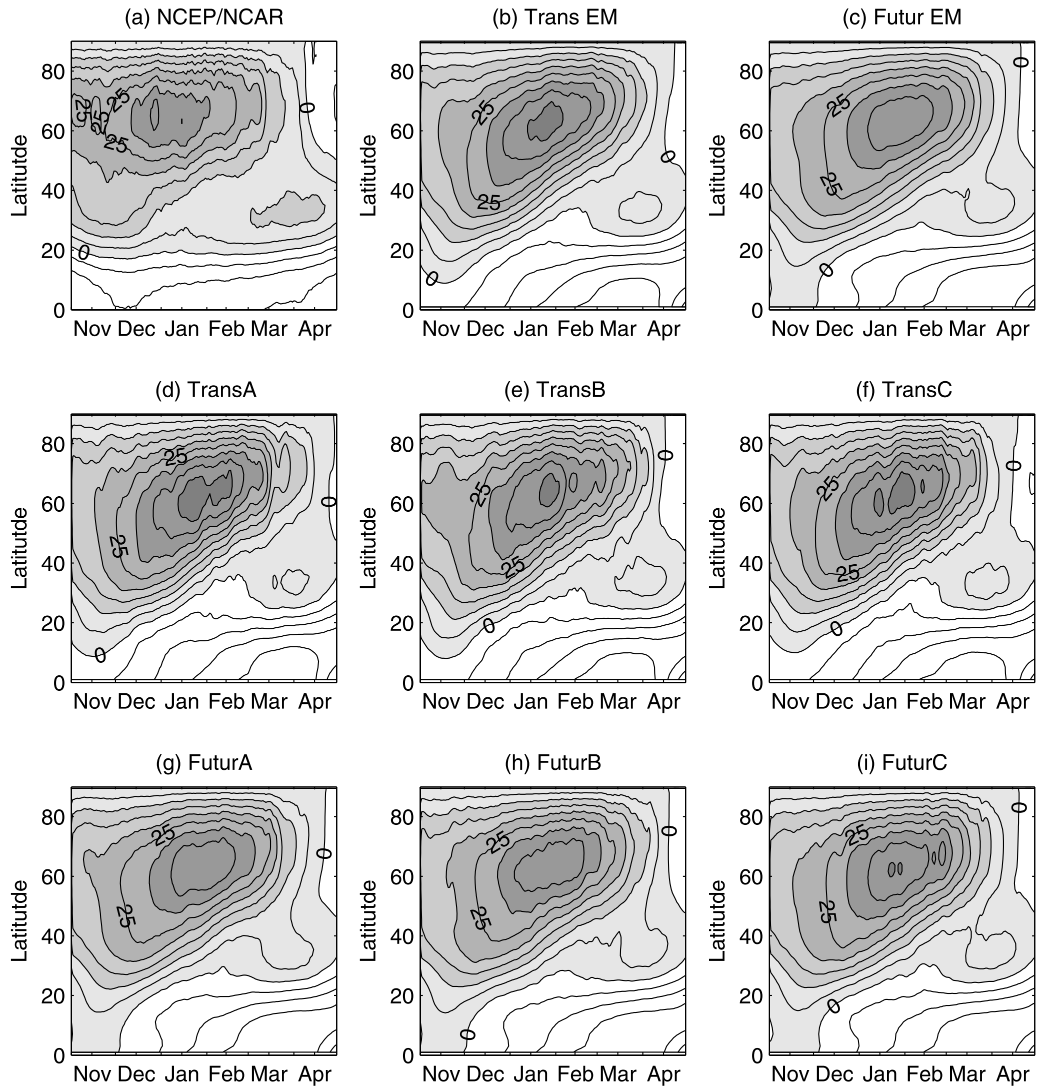

Figure 1. Zonal mean zonal wind climatology of models at 10 hPa for the (a) NCEP/NCAR, (b) TRANS ensemble mean, (c) FUTUR ensemble mean, and (d–i) individual members. Contour interval is 5 ms^{-1}. Positive values are shaded.

GFDL coupled chemistry climate model AMTRAC. These runs include significant changes to both greenhouse gas concentrations and chlorofluorocarbon concentrations needed to determine the ozone distribution in the stratosphere. Our aim is to examine whether there is a detectable difference in the number, seasonal distribution and dynamics of SSWs between simulations of the late 20th and those of 21st century.

[6] One early obstacle to quantifying possible changes to the frequency and characteristics of SSWs was the lack of a standardized basis for comparing model results to observations. This situation has been remedied, to a large degree, by our recent work [*Charlton and Polvani*, 2007; *Charlton et al.*, 2007]. In those papers a set of benchmarks, based on both the NCAR/NCEP and ERA-40 reanalyses, was defined; the proposed methodology was then applied across 6 stratosphere-resolving GCMs, to determine the degree with which each model was able to reproduce the observed climatology. The same methodology will be used in this paper, but with a different goal: the detection of possible changes in SSW properties over the coming century.

2. Model and Methodology

2.1. Model

[7] In this paper we analyze output from simulations of the GFDL (Geophysical Fluid Dynamics Laboratory) coupled chemistry climate model AMTRAC (Atmospheric Model With Transport and Chemistry); other aspects of these integrations have been reported previously in a number of studies [*Austin and Wilson*, 2006; *Austin et al.*, 2007; *Li et al.*, 2008]. Briefly, AMTRAC has 48 levels in the vertical, with the model top at 0.002 hPa; its horizontal resolution is 2° latitude by 2.5° longitude. The model's parameterizations are identical to those in the GFDL GAMDT model [*GFDL Global Atmosphere Model Development Team*, 2004], except for the gravity wave drag used in the Middle Atmosphere (which is represented using the

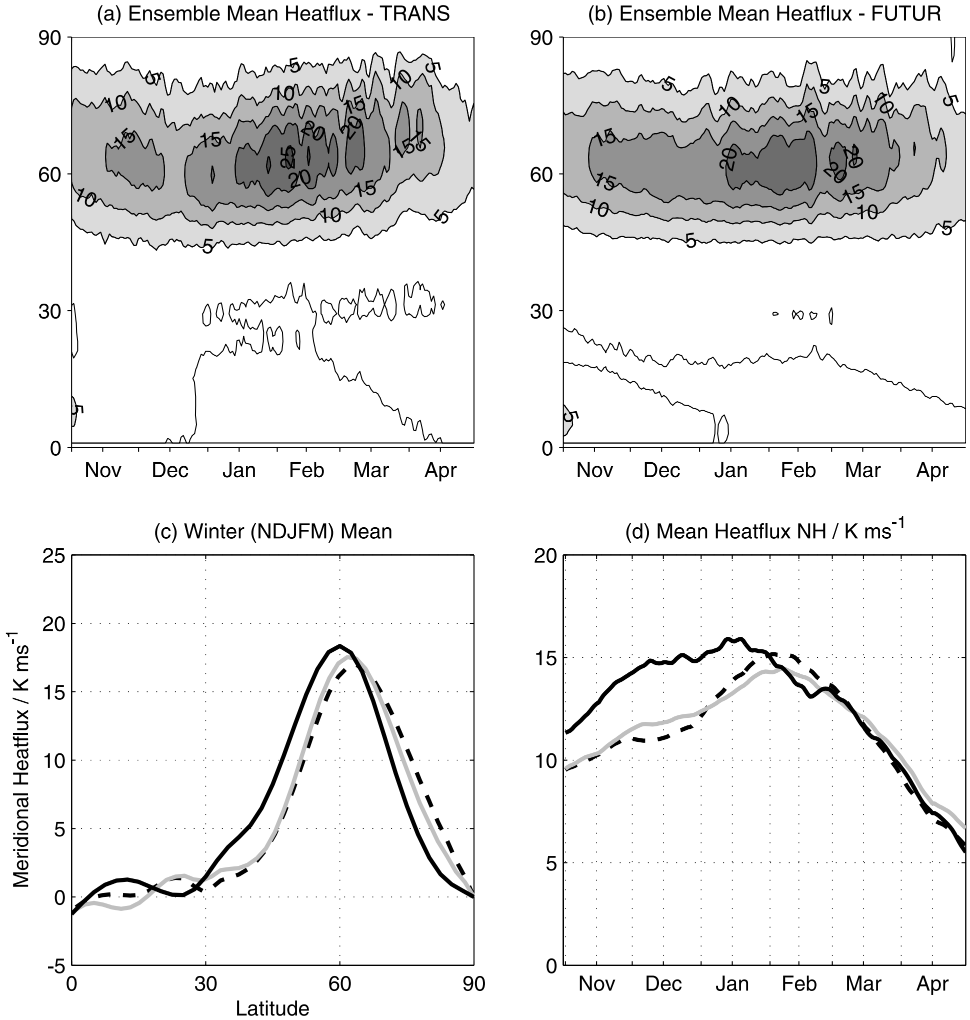

Figure 2. Meridional heat flux climatology at 100 hPa for (a) the TRANS ensemble mean and (b) the FUTUR ensemble mean. Contour interval at 5 K ms^{-1}. (c) Winter mean (NDJFM) meridional heat flux in the NCEP/NCAR reanalysis (solid line), TRANS EM (dashed line), and FUTUR EM (gray line). (d) Climatological meridional heat flux, integrated from 45°N to the pole, versus day of the year, smoothed with a 31-day running mean; line styles as in Figure 2c.

scheme of *Alexander and Dunkerton* [1999]). Comprehensive stratospheric chemistry and somewhat simpler tropospheric chemistry (CH_4 oxidation plus additional reactions) are also included.

[8] Two ensembles of runs are compared here: one ensemble simulates the observed climate between 1960 and 2004 (this is referred to as the TRANS ensemble, or simply the "recent past"). The other ensemble simulates recent and future climate between 1990 and 2099 (this is the FUTUR ensemble, or simply the "future"). Each ensemble is composed of three members. The number and length of the runs, a total of 420 years, makes a comprehensive study of simulated stratospheric variability in the recent past and future possible.

[9] The TRANS simulations are initialized from different years of a control time-slice integration of the model, which

Table 1. SSWs in the AMTRAC Integrations and the NCEP/NCAR Reanalyses

Simulation	No. of Winters	No. of Events	No. of Vortex Displacements	No. of Vortex Splits	SSW Frequency, Events/Decade	SSW Type, Displacement/Splitting
TRANS A	45	16	12	4	3.6	3.0
TRANS B	45	15	11	4	3.3	2.8
TRANS C	45	12	8	4	2.7	2.0
TRANS Mean	135	14.3	10.3	4.0	3.2	2.6
FUTUR A	110	42	32	10	3.8	3.2
FUTUR B	110	46	39	7	4.2	5.6
FUTUR C	110	44	35	9	4.0	3.9
FUTUR Mean	330	44.0	35.3	8.7	4.0	4.1
NCEP/NCAR	45	27	15	12	6.0	1.3

Table 2. Significance Tests of SSWs in the TRANS Runs of AMTRAC Versus Those in NCEP/NCAR Reanalyses[a]

Simulation	Expected Value of Events/Decade	Standard Error	Different from NCEP at 0.10	Different from NCEP at 0.05
TRANS A	3.6	0.8	yes	no
TRANS B	3.3	0.8	yes	yes
TRANS C	2.7	0.7	yes	yes
TRANS mean	3.2	0.4	yes	yes

[a]Note that TRANS integrations are over approximately the same period as the NCEP/NCAR reanalysis.

used fixed concentrations of greenhouse gases (GHGs), chlorofluorocarbons (CFCs) and aerosols at 1960 levels. The model is then forced with observed, time-dependent climate forcings representing GHGs, CFCs aerosols and solar forcing. Time-dependent, observed sea surface temperatures (SSTs) and sea-ice amounts are used.

[10] The FUTUR runs are initialized from the corresponding 1 January 1990 of the TRANS runs. The SST and sea-ice amount is taken from a simulation of the coupled atmosphere-ocean version of the GFDL model, but with limited vertical domain (simulation 2.1, *Delworth et al.* [2006]). The GHG forcings are taken from Intergovernmental Panel on Climate Change (IPCC) scenario A1B [*Houghton et al.*, 2001, Appendix II] and CFC forcings are taken from the World Meteorological Organisation (WMO) Scientific Assessment of Ozone Depletion *WMO* [2003, chapter 1], reference profile A1.

[11] We recognize the inherent difficulty in trying to infer changes to a highly variable and perhaps poorly simulated component of the climate system using only a single CCM. GCMs and CCMs vary widely in their ability to simulate the frequency and climatology of SSWs. Hence some caution is in order. The CCM analyzed in this paper is chosen, in particular, because a number of ensemble members and relatively long integrations are available, when compared to other data sets.

2.2. Methodology

[12] In this paper, we closely follow the procedure outlined in our previous studies for detecting and classifying SSWs [*Charlton and Polvani*, 2007]. To summarize, SSWs are defined to occur when the zonal mean zonal winds at 10 hPa and 60°N become easterly, during the winter season, from November to March. In addition, two criteria are used to avoid overestimating the number of midwinter SSWs. First, to avoid double counting, we check if a previous SSW has been recorded in the 20 immediately preceding days. Second, to ensure that final warmings are not counted, we remove events for which the zonal mean zonal winds at 10 hPa and 60°N do not return to westerly values for 10 consecutive days following the SSW.

[13] Once the events are identified, a further procedure is used to classify the events as vortex displacement type SSWs (in which the vortex shifts off the pole) or vortex splitting type SSWs (in which the vortex breaks up into large, similarly sized, pieces). The algorithm we use is somewhat complex, and combines diagnosis of absolute vorticity, as a surrogate of potential vorticity, with techniques used in early computer vision studies to describe the edge of the polar vortex. Beyond the frequency and type of events, we also look at the characteristics of SSWs in the model simulations by comparing them to the benchmarks we have previously established. The benchmarks describe the degree to which polar temperatures increase, the deceleration of the zonal mean wind at the vortex edge and the amount of meridional heat flux in the lower stratosphere preceding each SSW. Detailed description of the calculation of each benchmark is given in section 4.

[14] Climatological information about SSWs is derived from the NCEP/NCAR (National Centers for Environmental Prediction/National Center for Atmospheric Research) reanalysis [*Kistler et al.*, 2001], between 1958 and 2001. Previous results clearly indicate that there is little difference between SSWs in the NCEP/NCAR reanalysis and in the ERA-40 Reanalysis (from the European Centre for Medium-Range Weather Forecasts).

[15] In several instances below we refer to the "ensemble mean" of a given diagnostic quantity: in all cases this is computed as follows. Each diagnostic quantity is first

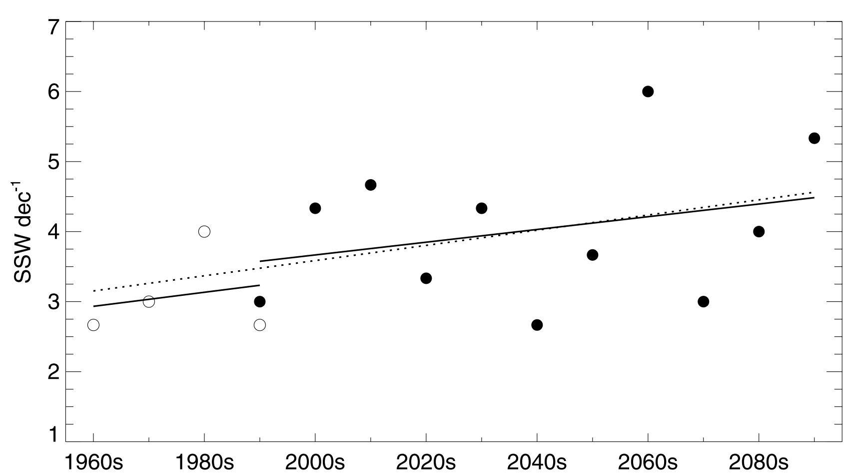

Figure 3. Ensemble mean number SSWs in each decade of the TRANS run (open circles) and the FUTUR run (solid circles). Linear regression lines for the TRANS and FUTUR runs (solid lines) and for the combined runs (dotted lines) are also shown.

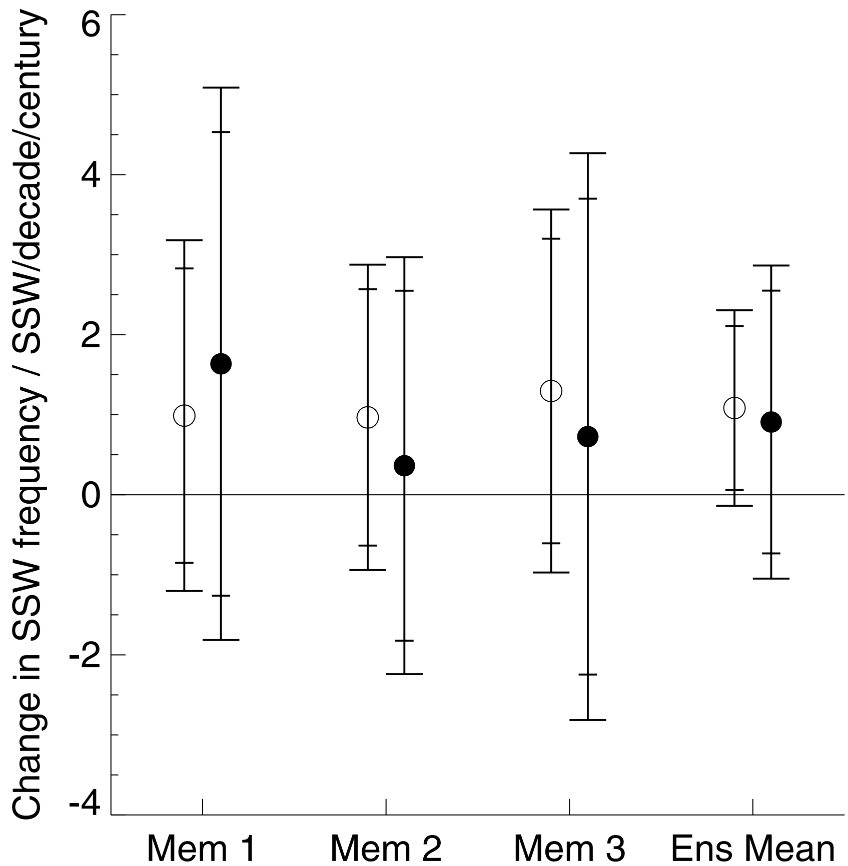

Figure 4. Linear trend in SSW/decade/century in each or the three ensemble members and for the ensemble mean. Open circles show the trend for the combined runs, and solid circles show the trend for the FUTUR runs. Solid lines represent 90% and 95% confidence intervals, marked by small and cross bars, respectively.

calculated for each member of the ensemble, and then the mean of the diagnostic across the ensemble is taken.

3. AMTRAC Model Climatology

[16] Before examining in detail the SSWs found in the model integrations it is useful to start by taking a brief look at the model's climatology of the middle stratosphere itself. First we consider the simulated zonal winds. The zonal mean zonal wind climatology, for each of the model runs discussed in this paper, is shown in Figure 1. The TRANS ensemble simulations compare well with the NCEP/NCAR reanalysis. The zonal mean zonal wind jet is slightly stronger in both the TRANS and FUTUR integrations compared to the reanalysis, particularly in the TRANS ensemble, but shows the same drift toward the pole during winter, including the double jet structure toward the end of March. Other than for a slight weakening of the polar vortex (also reported by other studies), there is little difference in the structure of the zonal mean zonal winds at 10 hPa in the FUTUR ensemble, either in any individual member or in the ensemble mean. Comparison of the two zonal mean zonal wind climatologies shows a small broadening or shift equatorward of the stratospheric jet in the FUTUR ensemble (not shown).

[17] Second, we consider the meridional heat flux at 100 hPa, which is a proxy for Rossby wave flux entering the stratosphere. The climatology of meridional heat flux in the two ensembles is shown in Figure 2: as for the zonal mean zonal wind, there is little difference between the TRANS and FUTUR integrations. Comparison of the winter mean heat flux, lower left panel, shows that wave flux peaks around 60°N and extends over approximately the correct range of latitude, in comparison with the heat flux climatology of the NCEP/NCAR reanalysis.

[18] One deficiency in our model integrations for both the recent past and the future is the lack of meridional heat flux

Table 3. SSWs in the Period 2055–2099 in the AMTRAC Integrations of Future Climate

Simulation	No. of winters	No. of events	No. of vortex displacements	No. of vortex splits	SSW Frequency, Events/Decade	SSW Type, Displacement/Splitting
FUTUR A	45	19	15	4	4.2	3.8
FUTUR B	45	21	16	5	4.7	3.2
FUTUR C	45	21	16	5	4.7	3.2
FUTUR mean	135	20	15.7	4.7	4.5	3.4

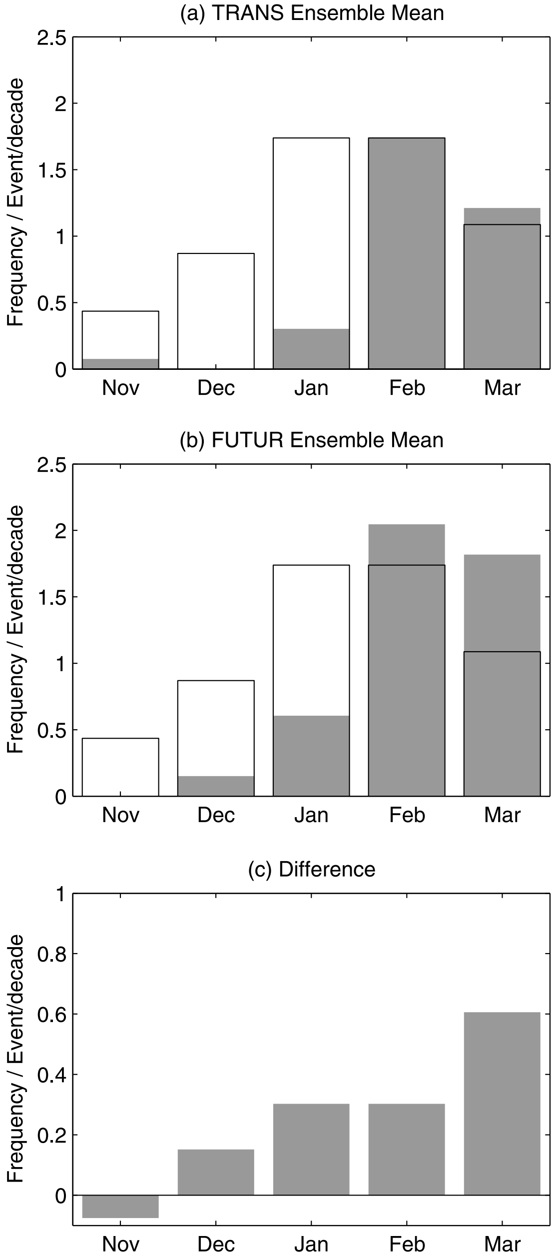

Figure 5. Seasonal distribution of stratospheric warmings by month in NCEP/NCAR reanalysis (open bars) and AMTRAC ensemble means (gray bars). Figure 5a shows TRANS runs for the period 1960–2004. Figure 5b shows FUTUR runs for the period 2055–2099. Figure 5c shows difference between two ensembles.

in early to midwinter (November to January), as can be seen in the bottom right panel of Figure 2. This is probably the reason for a somewhat low number of SSWs during the same period in both ensembles, as we will demonstrate in the next section.

4. Frequency of SSWs Under Anthropogenic Climate Change

[19] The first major component of this study consists of assessing whether changes in the frequency of SSWs appear in the model simulations as a consequence of anthropogenic forcings, and in determining whether such changes are statistically significant. In this section we present two different methods for determining the size and significance of changes in SSW frequency over the recent past and the 21st century. First, we compute the trend in SSW frequency over the entire length of the two ensembles. Second we contrast the simulations of the recent past with a period of comparable length at the end of the future simulations. Using these two distinct methods and comparing their results lends confidence that our results are robust and not simply an artifact of the analysis method used.

[20] The SSW statistics for all model integrations are shown in Table 1. The key numbers in this table are the frequency of events per winter season and the type of events, expressed as the ratio vortex displacement events to vortex splitting events. These numbers, given in the last two columns of the table, should be compared to those extracted from the NCEP/NCAR reanalyses; the latter shows an SSW frequency of 6.0 events/decade and a type ratio of 1.3 vortex displacements for each vortex split. A statistical test, allowing the differentiation between CCM integrations and the reanalysis data set for a single CCM realization in terms of the frequency of SSWs was outlined in the Appendix of *Charlton et al.* [2007]. Results from applying that test for the TRANS ensemble members and their total ensemble with the NCEP/NCAR reanalysis climatology are shown in Table 2. Clearly AMTRAC, as most other current generation GCMs, is unable to accurately simulate the frequency of SSWs in the recent past.

[21] As is shown in section 5, a large part of the discrepancy between modelled and observed SSW frequencies is due to a large deficit in the number of vortex splitting SSWs in AMTRAC. As a point of comparison, in our previous study of six stratosphere-resolving GCMs it was found that five of the six simulated fewer SSWs than the NCEP/NCAR climatology. The multimodel ensemble mean frequency of SSWs for the six models was 3.9 events per decade. Hence the SSW frequency in the TRANS simulations of AMTRAC is typical of current generation GCMs. While this relatively low frequency may be a cause of concern in terms of the model's predictions for future climate, we nonetheless proceed in computing trends in SSW frequency, and return to this point in the discussion section below.

4.1. Trend in SSW Frequency

[22] First, the trend in SSW frequency across the two ensembles of integrations is computed. SSW data from each of the model integrations are divided into decadal frequency bins, thereby reducing some of the noise in the frequency data. Figure 3 shows the ensemble mean frequency of SSWs for each decade of the model runs, along with a linear regression fit to the two ensembles separately (solid lines) and to a combined ensemble; for the latter, members are constructed by joining the first three decades of each TRANS run with the corresponding FUTUR run. Each ensemble member can be thought of as a single integration, since the initial conditions for the three FUTUR integrations are taken from the 1 January 1990 state in each of the three TRANS runs. Taking the ensemble mean removes some of the model variability, and allows us to see clear evidence for an upward trend in SSW frequency in the model. Note that

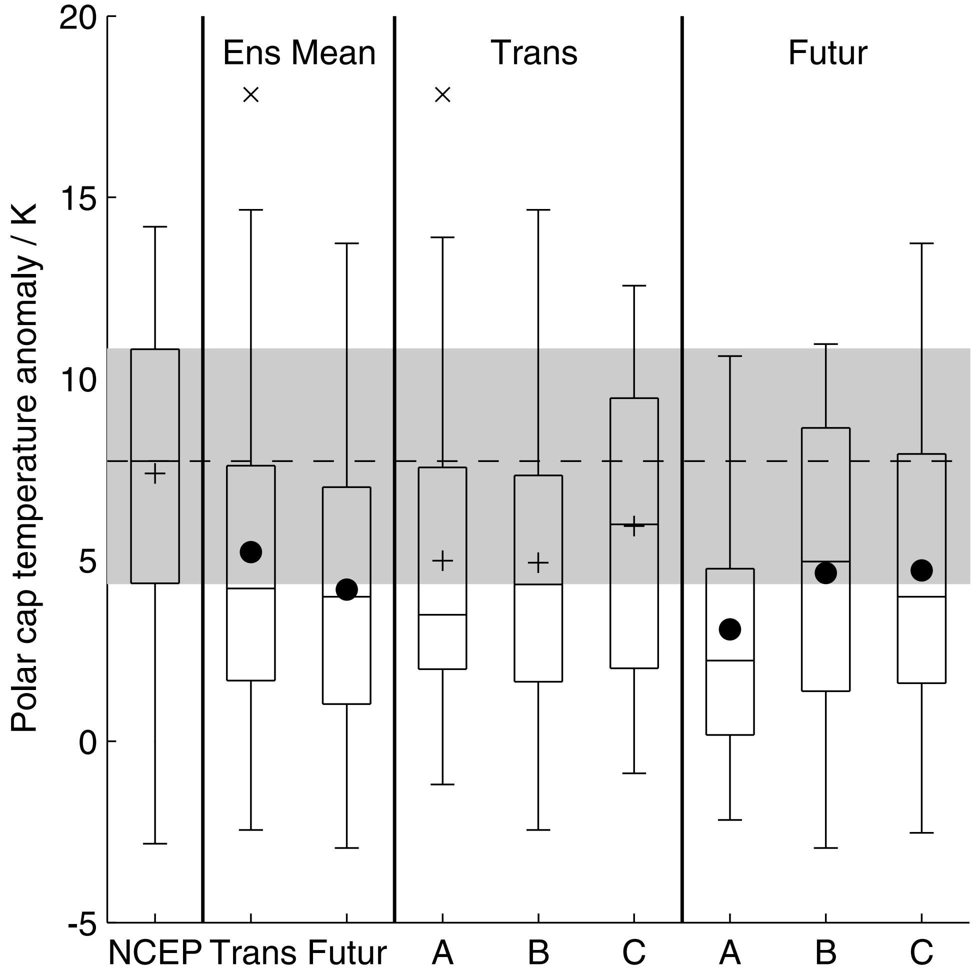

Figure 6. The distribution of mean polar cap temperature anomalies at 10 hPa (90–50°N) for SSWs in the TRANS and FUTUR ensembles and the NCEP/NCAR reanalysis. Box plots show interquartile range with a box, the median as a solid line parallel to the *x* axis at the center of each box and the data range in the lines parallel to the *y* axis starting at the edges of the box. Outliers are marked by an "x". The arithmetic mean for SSWs in each model or data set is shown by a cross. Gray shading shows interquartile range of reanalysis, and dashed thin line shows median of reanalysis. If the mean of the quantity for a run is significantly different from the mean of the same quantity in the NCEP/NCAR reanalysis, the cross is replaced by a solid circle.

the trend is roughly the same in the TRANS, the FUTUR and the combined ensembles. This trend consists of an increase in frequency of 1 event/decade by the end of the 21st century (i.e., the trend in the AMTRAC integrations is, approximately, 1 event/decade/century).

[23] Figure 3 also gives a clear indication that the interdecadal variability in SSW frequency is quite large; this is well known, in both models and observations [cf. *Butchart et al.*, 2000; *Charlton et al.*, 2007]. The large interannual variability makes the estimation of a reliable trend in SSW frequency difficult to establish in a statistically significant manner.

[24] The statistical significance for our AMTRAC integrations is summarized in Figure 4, which shows the linear trend in each of the three experiments and the 90 and 95% confidence limits for each estimate. Open dots show the estimate for the combined runs and filled dots show the estimates for the FUTUR runs only. The difficulty in assigning statistical confidence to trends in SSW frequency is highlighted by the considerable variability in the trend estimate among the three ensemble members. Taking the ensemble mean reduces some of this uncertainty: the confidence intervals for the two-ensemble mean estimates are both smaller.

[25] For the combined runs, we are able to obtain a trend of 1.1 event/decade/century which is statistically distinct from zero. As far as we are aware, this is the first time that a significant positive trend in SSW frequency has been demonstrated in a transient simulation of the 21st century.

4.2. Difference in SSW Frequency Between 1960–2004 and 2055–2099

[26] A second way to establish the presence of a trend in SSW frequency is to consider the differences in SSW

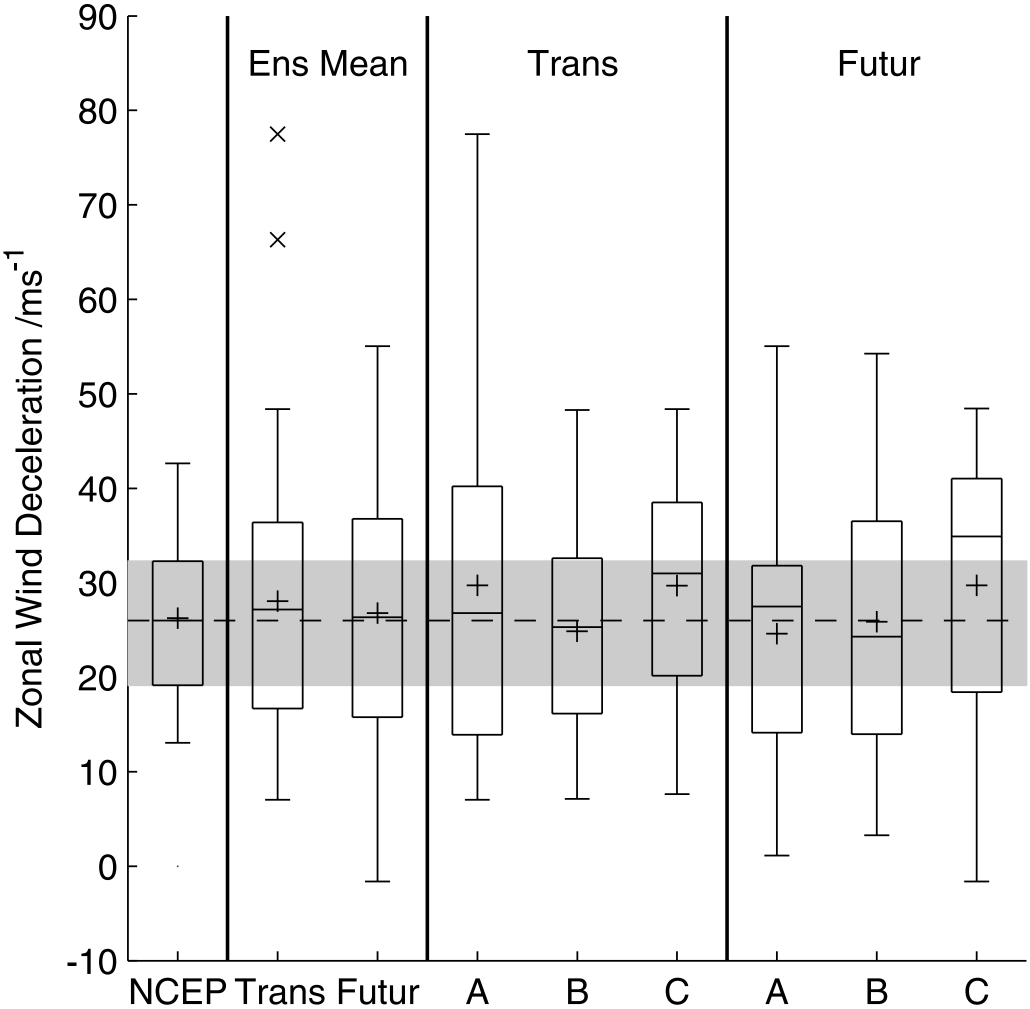

Figure 7. As in Figure 6 but for zonal mean zonal wind deceleration.

frequency between the recent past simulations (TRANS) and a comparably long interval at the end of the 21st century. To do this, the period at the end of the FUTUR runs between 2055 and 2099 is compared to the TRANS ensemble (which has a similar length). The results are shown is shown in Table 3.

[27] The ensemble mean frequency of SSWs at the end of the FUTUR run is 4.6 events/decade, a relatively large increase in SSW frequency compared the values of 3.2 event/decade in the TRANS ensemble. This increase is comparable to the trend in SSWs apparent in Figure 3. Furthermore, it is statistically significant at both the 0.10 and 0.05 confidence levels using the statistical test outlined in *Charlton et al.* [2007].

[28] In summary we conclude that, although SSW trends are difficult to measure owing to a large interannual variability, the AMTRAC simulations predict a positive, small, yet statistically significant increase in the frequency of sudden warmings by the end of the 21st century.

[29] One note of caution regarding this conclusion. The specification of SST in the TRANS and FUTUR runs is quite different. There is no easy way of estimating whether this has a direct effect on SSWs and their frequency. Nonetheless, this difference and its possible effect are something which needs to be explored in future studies.

5. Changes to SSWs Properties Under Anthropogenic Change

[30] Given the predicted increase in frequency of SSWs, one is led to consider whether the dynamics of these events might also be different in future climates. This question is addressed next. In order to bring out possible differences in the clearest way, all diagnostics in this section are applied to SSW events which occur after 2055 in the FUTUR integrations, by which time a change in the frequency of SSWs is statistically significant.

5.1. Types of SSWs

[31] We start by exploring whether the ratio of the number of vortex displacement to vortex splitting events is different in the future climate. Recall that, in the NCEP/NCAR reanalyses, this ratio is found to be 1.3 vortex displacement events for each vortex splitting event.

[32] As can be seen in Table 1, considering first SSW events in all the TRANS ensemble together, we find a total

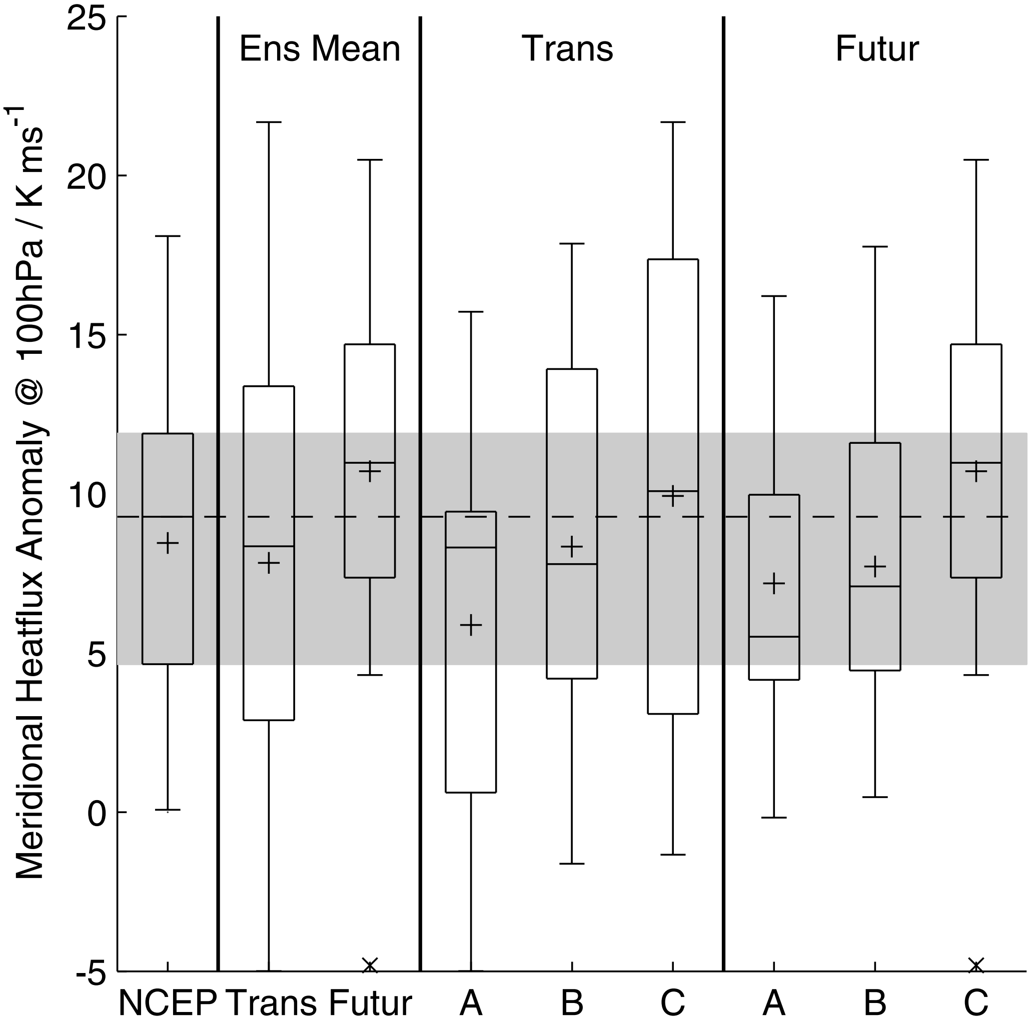

Figure 8. As in Figure 6 but for meridional heat flux.

of 31 vortex displacement events and 12 vortex splitting events, yielding a mean ratio of 2.6. Hence AMTRAC appears unable to capture the observed ratio in climate of the recent past. While perhaps disappointing, it is important to realize that for most GCMs this ratio is larger than the reanalysis value [*Charlton et al.*, 2007]. However, because of the inherent uncertainty in its estimation, this value cannot be said to be significantly different to the value in the reanalyses.

[33] Applying a similar statistical test, one may next compare the ratio of vortex displacement and splitting events in the TRANS ensemble with the ratio in the final half of the FUTUR ensemble. We find the latter to be 3.4 and, again, this is not significantly different to the ratio in TRANS ensemble. The CCM experiments, therefore, predict no statistically significant difference in the type of SSW in the 21st century.

5.2. Seasonal Distribution of SSWs

[34] We next consider the seasonal distribution of SSWs. Figure 5 shows the ensemble mean frequency of SSWs in the TRANS ensemble and the second half of the FUTUR ensemble as a function of month of the extended winter. It is immediately obvious that there are some deficiencies in the model's simulation of SSWs, particularly a lack of SSW activity in the early months of winter. This can be traced back to the meridional wave flux climatology (Figure 2) which shows a lack of Rossby wave activity in early winter in the model. Nevertheless, the climatologies are instructive in that they allow a comparison of the seasonality of SSW activity in the two sets of scenarios.

[35] Changes to SSW frequency are largest toward the end of winter and smallest at the beginning of winter. There is an almost 50% increase in SSW frequency in March in the second half of the FUTUR ensemble. Recall that none of these late events are final warmings, as those are excluded by our methodology. It is impossible to determine if this large change in SSW frequency at the end of winter is due to a change in the dynamics of the polar vortex or simply a reflection of the inability of AMTRAC to simulate an accurate number of SSWs in early winter. Closer inspection of Figure 2 shows that there are small changes to the amount of meridional heat flux over the seasonal cycle (10% less heat flux in December and 10% more heat flux in February and March in the FUTUR runs) which might provide a partial explanation of the changes in seasonality.

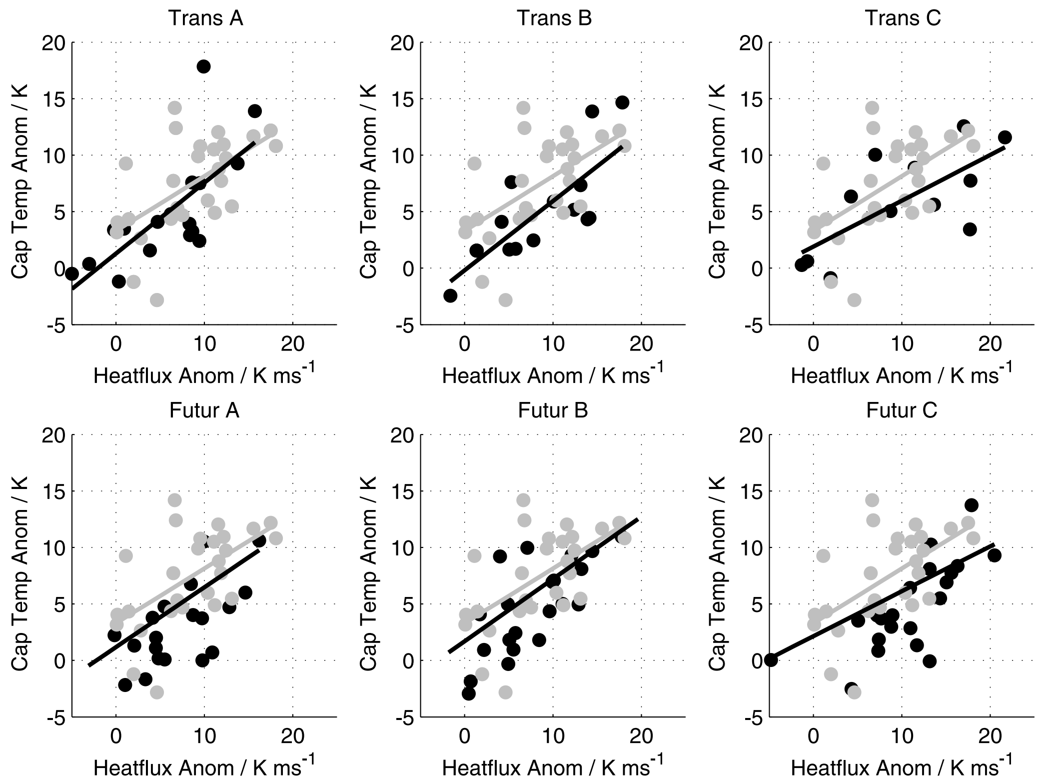

Figure 9. Polar cap temperature versus meridional heat flux benchmarks associated with SSW events in the (top) TRANS and (bottom) FUTUR runs. The corresponding values in the NCEP/NCAR reanalyses are shown in gray.

Additional experiments with dynamical and mechanistic models, where these changes to the seasonal heat flux are isolated would help to determine if they are responsible for the shift in SSW seasonality.

[36] It is also necessary to compare changes to heat flux and SSW climatology in many different GCMs and CCMs to confirm the robustness of this result. Previous authors have hypothesized about the existence of a trend in late winter, stratospheric radiative cooling, toward stronger cooling as carbon dioxide levels increase [*Pawson and Naujokat*, 1999]. A further cause of the trend toward late winter SSWs in our two sets of runs might be that the radiative cooling trend allows the vortex to recover faster in late winter, producing SSWs in the mid-21st century which might have become final warmings under current climate conditions.

5.3. Dynamical Properties of SSWs

[37] Finally, we examine some dynamical properties of SSWs in the AMTRAC simulations in order to assess whether any important change takes place as a consequence of anthropogenic forcing. In this study we focus on three of the dynamical benchmarks introduced by *Charlton and Polvani* [2007]. As is conventional, these diagnostics are referred to as process-based, because they consider the dynamical changes associated with the SSW process only, and do not include information about general stratospheric variability.

[38] The first benchmark gives an indication of the amplitude of SSWs in each integration. This benchmark is quantified by the area-weighted mean 10 hPa polar cap temperature anomaly, 90–50°N, 5 days from the onset date (denoted ΔT_{10}). Figure 6 shows box plots [*Wilks*, 2006, pp. 30–32] of ΔT_{10} for SSWs in each of the model integrations in the two ensembles, and an ensemble mean box plot which includes the process-based diagnostics for SSWs in all three ensemble members. In both the FUTUR and TRANS ensembles the amplitude of SSWs is significantly weaker than the SSWs in the NCEP/NCAR reanalysis data set. In addition all three FUTUR ensembles have SSWs with mean amplitude which is significantly weaker than SSWs in the NCEP/NCAR reanalysis data set. However, and this is the key point, there is no evidence of a change of amplitude of SSWs between the two TRANS and FUTUR integrations.

[39] The second benchmark relates to the change in westerly momentum that accompanies SSWs. It is quantified by the difference in zonal mean zonal wind, at 60°N and 10 hPa, 15–5 days prior to the onset date minus 0–5 days after the onset date (ΔU_{10}). Figure 7 shows box plots of ΔU_{10}. Again, there is little difference in ΔU_{10} between any of the model integrations or between the model integrations and the NCEP/NCAR reanalysis. This indicates that SSWs produce approximately the same change in westerly momentum in the climates of both ensembles.

[40] The third benchmark is used to understand the planetary wave activity that causes the SSWs in the model. This is quantified by the area-weighted, mean, 45–75°N, 100 hPa meridional heat flux anomaly from climatology, 20–0 days before the onset date ($\Delta\overline{v'T'_{100}}$). Figure 8 shows

box plots of $\Delta\overline{v'T'_{100}}$. As for the previous two benchmarks, there is little difference between any of the model integrations or between the model integrations and the NCEP/NCAR reanalysis. Very similar amounts of planetary wave flux are associated with SSWs in all of the climate simulations considered.

[41] Lastly, to examine the response of the stratosphere in each of the model integrations to fluxes of Rossby wave activity, we show scatter plots of ΔT_{10} against $\Delta\overline{v'T'_{100}}$ in Figure 9. In each case, the gray dots show SSWs in the NCEP/NCAR reanalysis and black dots show each model integration in turn. A linear fit to the data is indicated in the black and gray lines. As noted by *Charlton and Polvani* [2007] a significant and obvious relationship exists between these two benchmarks for the NCEP/NCAR reanalysis data, stronger heat flux before the SSW at 100 hPa is correlated with stronger warming of the polar cap at 10 hPa. This relationship is present in all of the model integrations, and all model integrations show a similar relationship between ΔT_{10} and $\Delta\overline{v'T'_{100}}$. This indicates that the sensitivity of the stratospheric state to inputs of Rossby wave flux is not noticeably changed by the increases of greenhouse gasses in the FUTUR ensemble.

[42] In summary, there is little to suggest that there is any change to the dynamics of SSWs in the FUTUR ensemble compared to the TRANS ensemble. Although there is some variability between the individual integrations in each case, there is no significant difference of any of the benchmarks between the two ensembles. In general, the dynamical properties of the SSWs compare well with SSWs in the NCEP/NCAR reanalysis data set, despite the fact that the model underestimates the frequency of events.

6. Discussion and Conclusions

[43] In this study we present an examination of changes to major, midwinter stratospheric sudden warmings between the 20th and 21st centuries. We compare two sets of transient model integrations, one with observed SSTs and climate forcings from 1960 to 2004 and one with predicted SSTs and climate forcings from the IPCC SRES A1B scenario. A statistically significant, small, positive trend amounting to 1.1 ± 0.6 events/decade/century is predicted over the 140 years of the simulation. In spite of this change in frequency, however, our model simulations suggest that the dynamical character of SSWs and the relative frequency of vortex displacement and splitting events will remain unchanged.

[44] One issue of concern is that the simulation of SSWs in our TRANS ensemble, which represents climate between 1960 and 2004, is significantly different from observed SSW variability in the NCEP/NCAR reanalysis over the same period. Low frequency of SSW occurrence in early winter is not an uncommon problem in GCMs [*Charlton et al.*, 2007]. An obvious extension to this work would be to perform a similar analysis to the one presented here over an ensemble of different CCMs, such as those used in CCMVal [*Eyring et al.*, 2006]. When such a study is undertaken, it will be important to characterize stratospheric variability both in the recent past and in the future to gain confidence in the predictions of the multimodel ensemble.

[45] There has also been much recent discussion in the literature about temperature trends in the polar lower stratosphere over the 21st century. Time-slice integrations tend to show a small positive temperature change at 100 hPa of the order of 0.5–1 K under doubled CO_2 conditions [*Rind et al.*, 1998; *Sigmond et al.*, 2004]. This change is explained either as an increase in the strength of the Brewer-Dobson circulation or in the frequency of SSWs. Previous studies using our integrations of AMTRAC [*Li et al.*, 2008] have shown that temperature trends in the lower stratosphere of the FUTUR runs are small and negative, −0.09K dec^{-1} north of 60°N at 100 hPa, consistent with other estimates from transient CCMs [*Eyring et al.*, 2006]. *Li et al.* [2008] also show an increase in the strength of the Brewer-Dobson circulation in these integrations of AMTRAC. Therefore neither increases in the strength of the Brewer-Dobson circulation nor increases in the frequency of SSWs lead to a positive temperature trend at 100 hPa in the 21st century in our model. It will thus be critical to confirm, in a large multimodel intercomparison such as CCMVal, what the trends in SSW frequency are and if changes in SSW frequency and trends in lower stratospheric temperatures are related.

[46] A useful byproduct of the analysis presented here is that an estimate of the computational resources required to determine trends in SSW frequency can be made. Because of the likely small size of this trend and the large interdecadal variability, 420 years of total simulation time were required to obtain a statistically significant result. This indicates that, if the amplitude of the trend simulated by our model is realistic, it will remain difficult to determine a significant trend in SSW frequency in observed atmospheric data for the foreseeable future, and that the SSW record will be dominated by natural internal variability throughout the 21st century.

[47] **Acknowledgments.** We thank Steven Pawson and two anonymous reviewers for insightful and helpful comments on the text. AJC-P is funded by a NERC Postdoctoral Fellowship Award NE/C518206/1. LMP is funded, in part, by the US National Science Foundation. JA's research was administered by the University Corporation for Atmospheric Research at the NOAA Geophysical Fluid Dynamics Laboratory. FL was supported by the Atmospheric and Oceanic Sciences postdoctoral program at Princeton University.

References

Alexander, M. J., and T. J. Dunkerton (1999), A spectral parameterization of mean flow forcing due to breaking gravity waves, *J. Atmos. Sci.*, *56*, 4167–4182.

Austin, J., and J. Wilson (2006), Ensemble simulations of the decline and recovery of stratospheric ozone, *J. Geophys. Res.*, *111*, D16314, doi:10.1029/2005JD006907.

Austin, J., J. Wilson, F. Li, and H. Vömel (2007), Evolution of water vapour concentrations and stratospheric age of air in coupled chemistry-climate model simulations, *J. Atmos. Sci.*, *64*, 905–921.

Baldwin, M. P., and T. J. Dunkerton (2001), Stratospheric harbingers of anomalous weather regimes, *Science*, *244*, 581–584.

Butchart, N., J. Austin, J. R. Knight, A. A. Scaife, and M. L. Gallani (2000), The response of the stratospheric climate to projected changes in the concentrations of well-mixed greenhouse gases from 1992 to 2051, *J. Clim.*, *13*, 2142–2159.

Charlton, A. J., and L. M. Polvani (2007), A new look at stratospheric sudden warmings. part I: Climatology and modelling benchmarks, *J. Clim.*, *20*, 449–471.

Charlton, A. J., A. O'Neill, W. A. Lahoz, and A. C. Massacand (2004), Sensitivity of tropospheric forecasts to stratospheric initial conditions, *Q. J. R. Meteorol. Soc.*, *130*, 1771–1792.

Charlton, A. J., L. M. Polvani, J. Perlwitz, F. Sassi, E. Manzini, S. Pawson, J. E. Nielsen, K. Shibata, and D. Rind (2007), A new look at stratospheric sudden warmings. part II: Evaluation of numerical model simulations, *J. Clim.*, *20*, 471–488.

Delworth, T. L., et al. (2006), GFDL's CM2 global coupled climate model. part I: Formulation and simulation characteristics, *J. Clim.*, *19*, 643–674.

Eyring, V., et al. (2006), Assessment of temperature, trace species and ozone in chemistry-climate model simulations of the recent past, *J. Geophys. Res.*, *111*, D22308, doi:10.1029/2006JD007327.

GFDL Global Atmosphere Model Development Team (2004), The new GFDL global atmosphere and land model am2/lm2: Evaluation with prescribed SST simulations, *J. Clim.*, *17*, 4641–4673.

Gillett, N., and D. W. J. Thompson (2003), Simulation of recent Southern Hemisphere climate change, *Science*, *302*, 273–275.

Gillett, N. P., M. R. Allen, and K. D. Williams (2003), Modelling the atmospheric response to doubled CO_2 and depleted stratospheric ozone using a stratosphere-resolving coupled GCM, *Q. J. R. Meteorol. Soc.*, *129*, 947–966.

Houghton, J. T., X. Ding, D. J. Griggs, M. Noguer, P. J. van der Linden, X. Dai, K. Maskell, and C. A. Johnson (Eds.) (2001), *Intergovernmental Panel on Climate Change 2001: The Scientific Basis. Third Assessment Report*, Appendix II, IPCC, Houghton, Cambridge, UK.

Kistler, R., et al. (2001), The NCEP-NCAR 50-year reanalysis: Monthly means CD-ROM and documentation, *Bull. Am. Meteorol. Soc.*, *82*, 247–267.

Li, F., J. Austin, and J. Wilson (2008), The strength of the Brewer-Dobson circulation in a changing climate: Coupled chemistry-climate model simulations, *J. Clim.*, *21*, 40–57.

Pawson, S., and B. Naujokat (1999), The cold winters of the middle 1990s in the northern lower stratosphere, *J. Geophys. Res.*, *104*, 14,209–14,222.

Rind, D., D. Shindell, P. Lonergan, and N. K. Balachandran (1998), Climate change and the middle atmosphere. part III: The doubled CO_2 climate revisited, *J. Clim.*, *11*, 876–894.

Scaife, A. A., J. R. Knight, G. K. Vallis, and C. K. Folland (2005), A stratospheric influence on the winter NAO and North Atlantic surface climate, *Geophys. Res. Lett.*, *32*, L18715, doi:10.1029/2005GL023226.

Sigmond, M., P. Siegmund, E. Manzini, and H. Kelder (2004), A simulation of the separate climate effects of middle atmospheric and tropospheric CO_2 doubling, *J. Clim.*, *17*, 2352–2367.

Wilks, D. S. (2006), *Statistical Methods in the Atmospheric Sciences*, 2nd ed., Elsevier, Burlington, MA.

WMO (2003), *WMO/UNEP Scientific Assessment of Ozone Depletion: 2002*, chap. 1, Report No. 47, World Meteorological Organisation, WMO Global Ozone Observing System, Geneva, Switzerland.

J. Austin, Geophysical Fluid Dynamics Laboratory, Princeton University, Forrestal Campus, 201 Forrestal Road, Princeton, NJ 08540–6649, USA.

A. J. Charlton-Perez, Department of Meteorology, University of Reading, P.O. Box 243, Reading RG6 6BB, UK. (a.j.charlton@reading.ac.uk)

F. Li, Goddard Earth Science and Technology Center, University of Maryland, Baltimore County, 5523 Research Park Drive, Suite 320, Baltimore, MD 21228, USA.

L. M. Polvani, Department of Applied Mathematics and Applied Physics, and Department of Earth and Environmental Sciences, Columbia University, New York, NY 10027, USA.